SolPol Measurement Sequence

ΕΘΝΙΚΟΝ ΑΣΤΕΡΟΣΚΟΠΕΙΟΝ ΑΘΗΝΩΝ
NATIONAL OBSERVATORY ATHENS

University of Hertfordshire UH

Contents

HEADER file details:

SOLAR POLARIMETER

1. Polarimeter Position [deg]
2. Rotator Position [deg]
3. PEM Setting [nm]
4. Retardation [waves]
5. Wavelength Filter (Wavelength-Bandwidth)
6. ND-Filter
7. Time (UTC)
8. Bias Voltage on Diode
9. LabJack, mean DC (AIN0)
10. LabJack, other
11. Lock-in, 1w
12. Lock-in, 2w

MEASUREMENT details:

- Measurement starts when **PEM** is @0° and **Polarizer** @41° (must always check on **solpol.exe** status board)
- File naming:
  pol_DDMMYYYY_HHMM_LOC_DURATION.txt
- where HHMM is the PC time, LOC is one of "antik", "ath" or "cy" for Antikythera, Athens and Cyprus data, respectively, and DURATION is the measurement duration as either "onehour", "twohours" or "sixteenmin".
- 5 measurements per polarizer position (~41°, 131°,221° and 311°) per assembly position (0° & 45°)
- Each measurement (4 Polarizer pos. – 1 PEM pos.) last ~4mins
- Ends ALWAYS with assembly at **45**°
- Total **2hrs file length** 8334 lines, where 160 hits should account for each polarizer position, size 91-92 Kb. The ½ goes for 1hr measurements.
- Full day measurement starts @6 UTC ends @16 to 16:15 UTC
- Dark measurements with shutter closed and instrument either in **Tracking** mode -> **poldarkT**, or **Non-Tracking** mode → **poldarkNT**
- Darks available only during Aug. – Sept. 2020 & 2021 datasets
- PEM aperture 23mm @ 90% efficiency
- Instrument FOV ~1° solid angle

MEASUREMENT sequence:

- Open **solpol.exe**, **picoscope.exe** and **opticstarview.exe** CCD camera program
- Hit the **Find** button in solpol.exe → wait for **"All peripherals found"** reading in the program screen
- Select in solpol.exe the **550nm** filter option and wait for Filter Wheel to operate (Picoscope indication varies)
- If sun appears on camera, polar alignment and parking positions are OK
- Slightly move the tracker to **N-S** & **E-W** directions through EQtab in order to target directly the Sun → maximization of the intensity signal in Picoscope voltage reading (reach at least 2.5 V & above if morning set-up)
- Hit track rate "Solar" (Sun icon) in EQtab and minimize tab
- Hit Initialize and wait for parameters
- Hit **Start** sequence → choose appropriate duration → save file and start (*wait for PEM to turn after 4'*)

SUN TRACKER Initialization & Tracking sequence:

Type: **EQ3 – SynScan** (lightweight, max. load of 10Kgs, less accurate in prolonged tracking) + **EQmod** direct PC control

- Open **CartesduCeil.exe** → Choose the appropriate observatory site, then → Telescope → Connect (Telescope EQtab opens)
- in EQmod tab → **Unpark** (co-ordinates scenario should be set to the specific instrument location)
- in **CartesduCeil.exe** search tab → Sun (Enter) → pointer on Sun (left click) → Telescope → Slew, tracker moves

Basic SolPol apparatus configuration

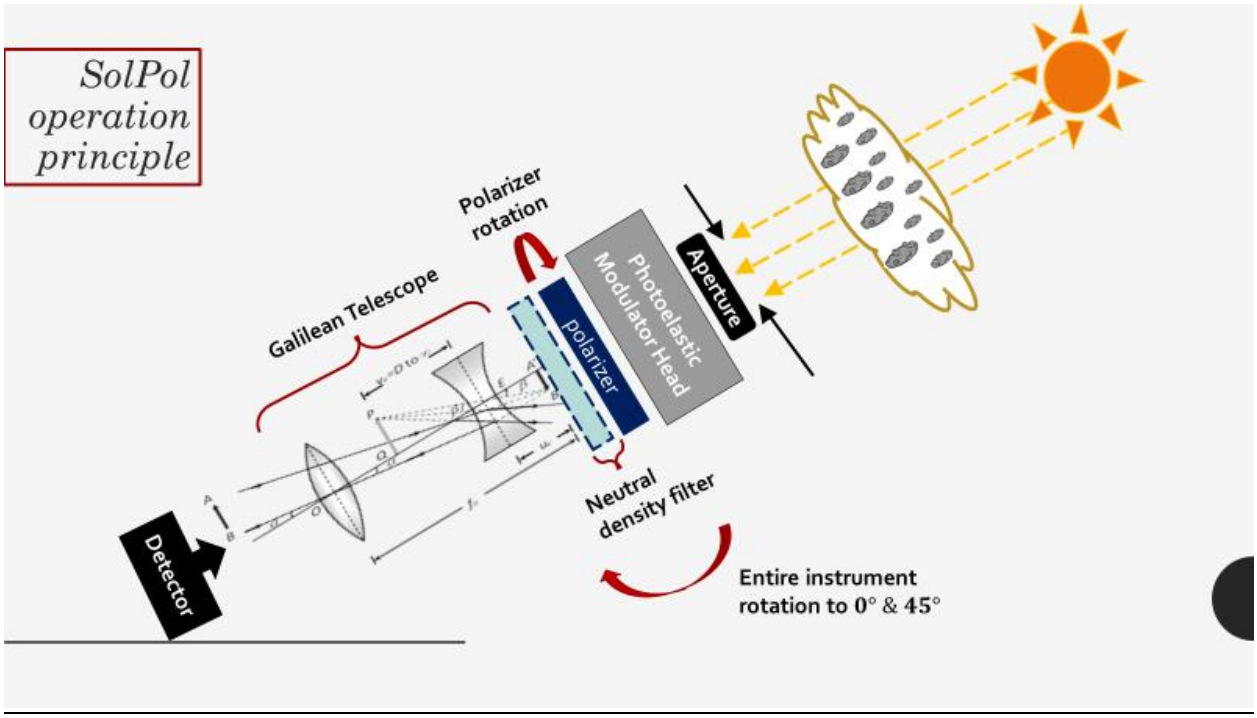

Instrument Set-up Antikythera

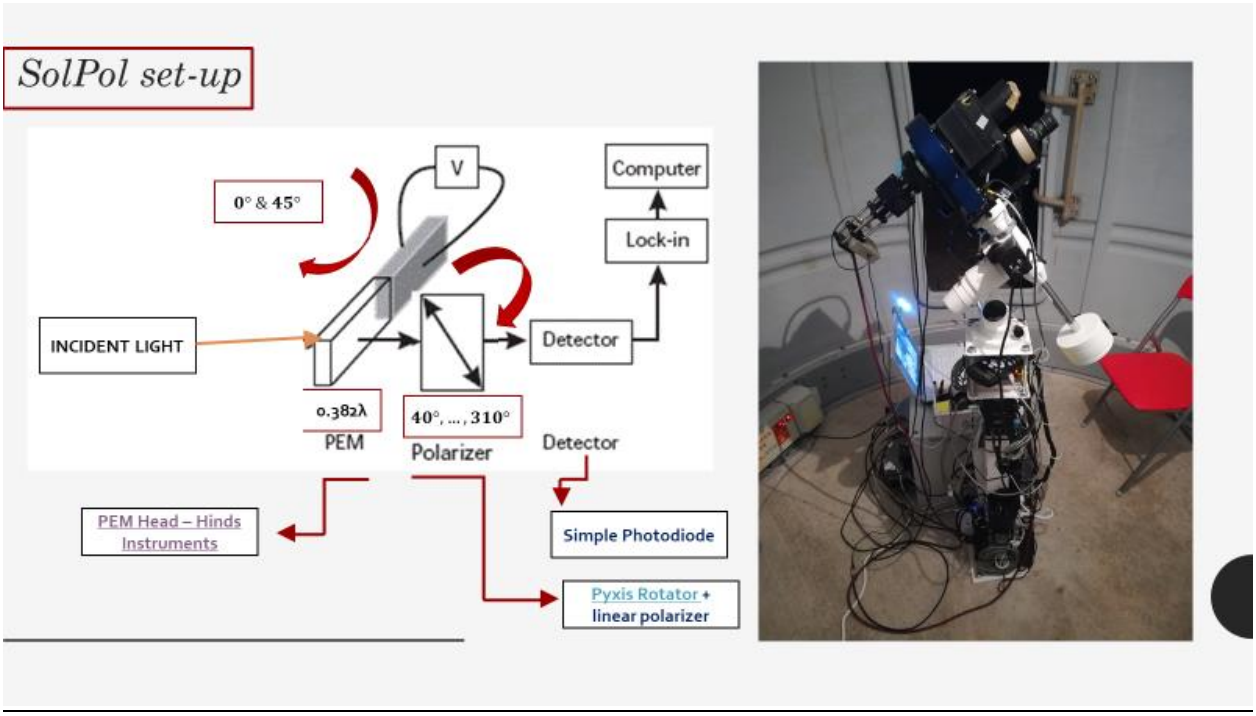

SolPol polarimeter includes a Photo Elastic Modulator (PEM) (47kHz PEM), a rotatable linear polarizer, an imaging telescope, neutral density filters, a field of view limiting aperture, and a large area diode detector (Martin et al., 2010). The design is quite a venerable one and follows the design of the PlanetPol instrument (Bailey et al., 2008;

 Instrument: *courtesy of the University of Hertfordshire*

Hough et al., 2006). The entire assembly can be rotated about the optical axis so that biases can be removed. The instrument measures the Stokes parameters that provide the linear and circular polarization from the whole solar disk plus a surrounding area of the sky depending on the choice of telescope and limiting aperture. Earlier measurements by Kemp with a nearly identical polarimeter design indicated that the whole solar disk has a linear polarization of ~ 10^{-6} from an observatory at 6300 ft altitude (Kemp et al., 1987; Kemp and Barbour, 1981).

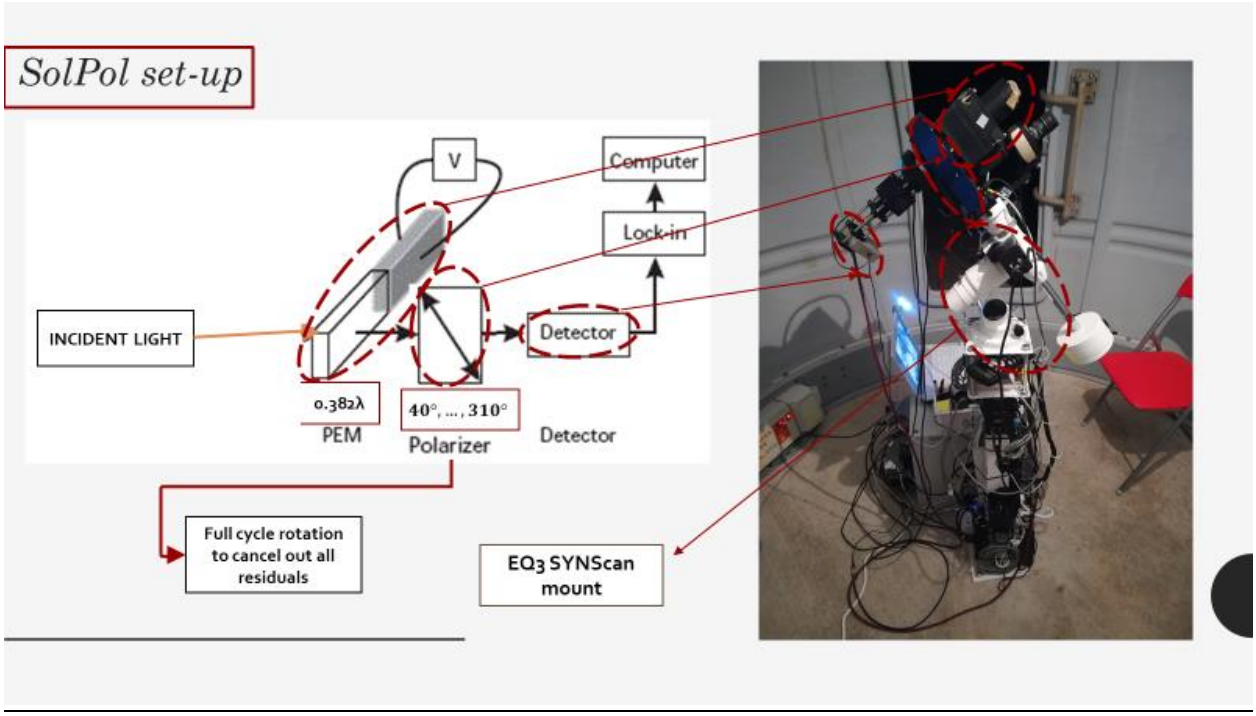

Figure 1 shows the basic SolPol design. There are no optical elements before the PEM (followed by the linear polarizer). Neutral density filters establish the signal levels at the 1cm silicon diode detector which uses a transimpedance amplifier to generate the signal voltage. The filter wheel contains six filters: RGB broad band filters (with measured transmission curves) and three 40nm narrow band filters at 400, 550, and 700nm centre wavelengths. The polarimeter currently operates at 550nm. A 12-bit A/D converter records the diode signal and an SR830 Lock-in amplifier records the first and second harmonic modulation signals (modulated by the PEM). The polarizer position and the instrument rotation are controlled from a LabView virtual instrument program, which also controls the recording of data from the detector.

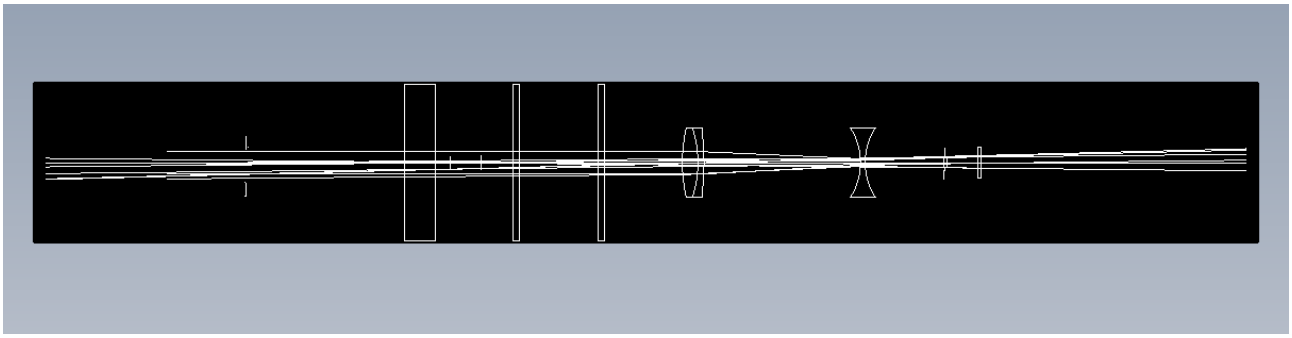

Figure 1: SolPol configuration. From left to right: 10mm aperture stop (as given for the initial configuration, but we've measured it in 5.5 mm in Antikythera), PEM, linear polarizer, neutral density filters, Lens 1 & 2 Galilean telescope, 3.5mm field stop, photodiode detector.

Instrument Parts and Specs

- Hinds Instruments – **Photoelastic Modulator (PEM)** Series II FS47, (Im. 1 in Fig. 2, **Optical head + Electronic head**)
  - Range: $\boldsymbol{400nm - 750nm}$
  - Cost: **(~12k £)**
- **Rotatable Linear Polarizer**, optical axis initially aligned with PEM axis
  - attached to Thorlabs Heavy Duty rotation stage (Im. 2 in Fig. 2)
  - rotated through a Thorlabs K-cube stepper motor controller
  - rotation controlled by the APT Thorlabs software

The linear polarizer is attached to a Heavy-Duty rotation stage, connected to the Pyxis rotator (front side) and glued to the PEM (Im. 2 in Fig. 2). For the polarizer rotation in 41°, 131°, 221°, 311° rotation, the stage is controlled by a Thorlabs Kinesis K-cube stepper motor (not depicted in the images in Fig. 2, as it is away from the main instrument bulk).

- Optec Inc. **PYXIS 3-inch camera field rotator** (Im. 3 in Fig. 2).

The Pyxis is a simple rotator used to attach CCD cameras on large telescopes for rotating the viewing field of the camera on long exposures. In SolPol it is used to rotate the entire instrument assembly from 0° to 45°.

- **NAUTILUS Rotating Filter Wheel** (Im. 4 in Fig. 2),
  - operation at $\boldsymbol{550\ nm}$
  - 7 available slots
- Galilean **Telescope** (Im. 5 in Fig. 2)
- Photodiode **detector** (also Im. 5 in Fig. 2)
- **CCD camera** for Sun tracking (Im. 6 in Fig. 2)
- Signal amplifier, through a transimpedance, SR830 DSP **Lock-In Amplifier** (Im. 7 in Fig. 2)
- PEM – 100 head controller unit (Im. 8 in Fig. 2)

 Instrument: ***courtesy of the University of Hertfordshire***

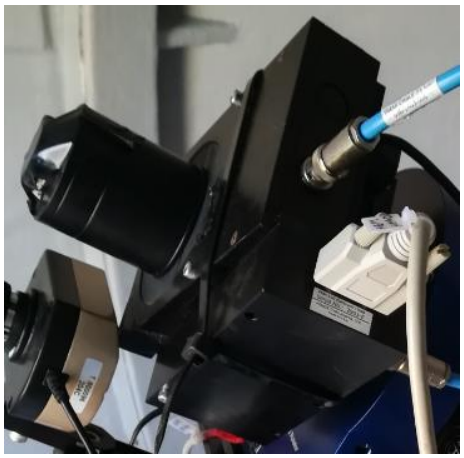

Im. 1

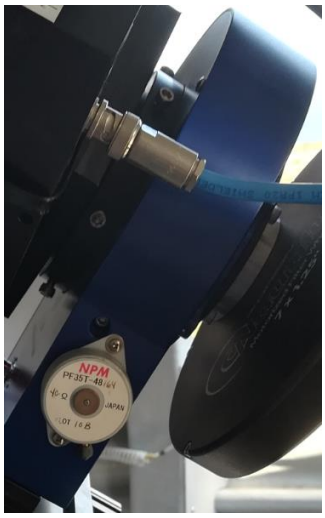

Im. 3

Im. 5

Im. 2

Im. 4

Im. 6

Im. 8

Im. 7

Figure 2: Instrument parts and peripherals. Im. 1: Photoelastic Modulator head (PEM), Im. 2: linear polarizer and Pyxis rotation stage, Im. 3: Pyxis camera (assembly) rotator, Im. 4: filter wheel, Im. 5: Galilean telescope and photodiode detector, Im. 6: CCD camera, Im. 7: Lock-in amplifier and Im. 8: PEM head controller.

 Instrument: ***courtesy of the University of Hertfordshire***

Photoelastic modulator (PEM) operation principle

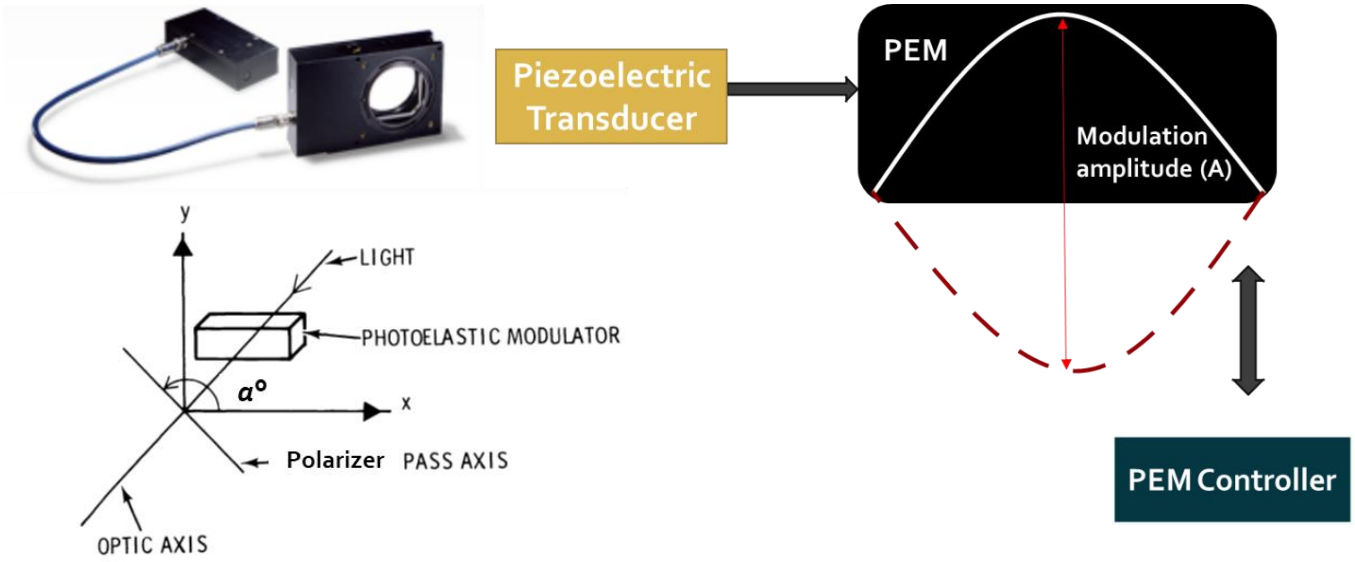

Figure 3: PEM assembly

The SolPol PEM SII FS47 is comprised of a fused silica crystal bar with photoelastic capabilities and a piezoelectric transducer. If the optical element is compressed or stretched it induces a retardation (i.e. phase difference between the polarization components) of the incoming light (Fig. 3). The strain stress in the PEM crystal is induced by standing mechanical acoustic waves, which are produced by the transducer, attached to the head. The resulting retardation is time-periodic, and is provided by:

$$\delta(t) = \mathrm{A}\sin\omega t \qquad \textbf{Eq. 1}$$

where δ is the retardation of the PEM and A is the peak amplitude. The resonant frequency ω of the PEM is set at 47 kHz.

The PEM controller unit performs many functions in the photoelastic modulator system. Its primary function is to control the peak retardation of the photoelastic modulator optical head. It does this by providing a DC voltage signal to the electronic head which determines the transducer vibration amplitude and thus the strain amplitude in the optical element. A current feedback loop from the electronic head enables the controller to maintain stable peak retardation levels.

For SolPol, the PEM is calibrated by the Bessel function zero methods (PEM User's manual, pg. 82). For the Bessel function zero method, the direct-current (DC) term is kept invariable, independent of the birefringence. The DC intensity also becomes independent of changes attributed to the optical system, such as angular position of the polarizer. Normalization of the AC signals by the DC signal, renders the ratio independent of fluctuations from the intensity source.

PEM specs

- **Fused siclica resonant bar** – initially non birefringent, stress-induced
- **Standing acoustic waves** imposed by transducer, at resonant freq. of **47kHz**
- Induced birefringence signifies that different polarization states are refracted on different directions
- **Fundamental vibration along the crystal optical axis** (Figs. 3; Stokes et al., 1976)
- According to the modulation amplitude, PEM can be used as any retardation plate between $\lambda/4$ *to* $\lambda/2$
- for 1ω the modulation efficiency is at 0.7342 and for 2ω at 0.6106, remains unchanged for dark measurements
- **PEM limitations:** mixing of linear & circular polarizations produced by residual strain in the fused silica (Stokes, R. A., 1976)

Instrument assembly rotation

The measurement sequence of SolPol includes the rotation of the whole instrument assembly by 0° and 45° (see measurements performed at 0° and 45° rotation in Table 1 of the following Section). The relative position of the PEM and linear polarizer for the instrument assembly rotation at 0° and 45° is shown in the following figure.

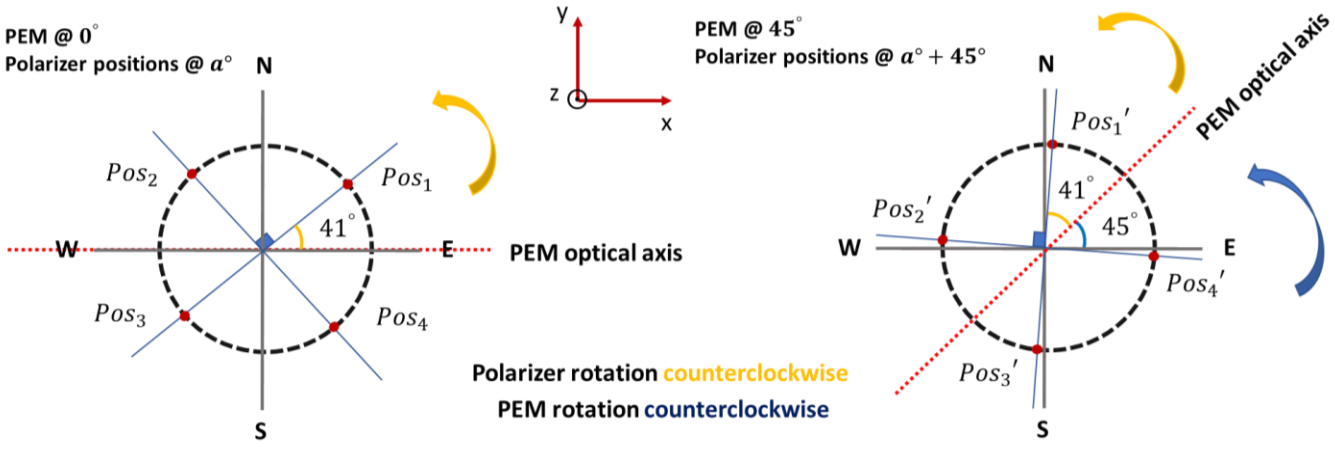

 Instrument: *courtesy of the University of Hertfordshire*

SolPol light modulation and measurements

The Mueller matrix of the PEM is:

$$\boldsymbol{M_{PEM}} = \begin{bmatrix} 1 & 0 & 0 & 0 \\ 0 & \mathrm{G} + \mathrm{H}\cos 4\psi & \mathrm{H}\sin 4\psi & -\sin\delta\sin 2\psi \\ 0 & \mathrm{H}\sin 4\psi & \mathrm{G} - \mathrm{H}\cos 4\psi & \sin\delta\cos 2\psi \\ 0 & \sin\delta\sin 2\psi & -\sin\delta\cos 2\psi & \cos\delta \end{bmatrix} \quad \textbf{Eq. 2}$$

with $\mathrm{G} = \frac{1}{2}(1 + \cos\delta)$ and $\mathrm{H} = \frac{1}{2}(1 - \cos\delta)$, $\delta = \mathrm{A}\sin\omega t$, ψ is the polarization position angle, i.e., the angle between the PEM optical axis and the produced parallel polarization component.

For the SolPol measurements $\psi = 0°$, thus Eq. 2 is written as Eq. 3.

$$\boldsymbol{M_{PEM,0^\circ}} = \begin{bmatrix} 1 & 0 & 0 & 0 \\ 0 & 1 & 0 & 0 \\ 0 & 0 & cos\delta & sin\delta \\ 0 & 0 & -sin\delta & cos\delta \end{bmatrix} \quad \textbf{Eq. 3}$$

The Mueller matrix for a rotating linear polarizer is (as in Freudenthaler 2016; S.10.8.2):

$$\boldsymbol{M_{Pol.,a^\circ}} = \frac{1}{2}\begin{bmatrix} 1 & cos2a & sin2a & 0 \\ cos2a & cos^2 2a & sin2acos2a & 0 \\ sin2a & sin2acos2a & sin^2 2a & 0 \\ 0 & 0 & 0 & 0 \end{bmatrix} \quad \textbf{Eq. 4}$$

Assembly without rotation

The Stokes vector of the light that reaches the detector is calculated as following:

$$\boldsymbol{I'_{\alpha^o}} = \boldsymbol{M_{Pol.,a^\circ} M_{PEM} I} = \frac{1}{2}\begin{bmatrix} I + Qcos2a + (Ucos\delta + Vsin\delta)sin2a \\ Icos2a + Qcos^2 2a + (Ucos\delta + Vsin\delta)sin2acos2a \\ Isin2a + Qsin2acos2a + (Ucos\delta + Vsin\delta)sin^2 2a \\ 0 \end{bmatrix} \quad \textbf{Eq. 5}$$

Using the Bessel functions (Eq.6), and omitting the terms higher than J_2, the intensity measured at the detector is provided by Eq. 7.

$$\cos\delta = \cos(\mathrm{A}\sin\omega t) = J_0(A) + 2J_2(A)\cos 2\omega t$$
$$\sin\delta = \sin(\mathrm{A}\sin\omega t) = 2J_1(A)\sin\omega t \quad \textbf{Eq. 6}$$

$$I'_{\alpha^o} = \frac{1}{2}I + \frac{1}{2}Q\cos 2a + \left[U\left[\frac{1}{2}J_0(A) + J_2(A)\cos 2\omega t\right] + VJ_1(A)\sin\omega t\right]\sin 2a \quad \textbf{Eq. 7}$$

Assembly rotated by 45^o

The whole assembly is rotated by 45^o, thus the reference coordinate system is rotated by 45^o. Then, the Stokes vector of the incoming sunlight appears in the new reference coordinate system to be rotated by an angle -45^o, and the Stokes vector $\mathbf{I_{rot}}$ is calculated using $\mathbf{R_{-45^\circ}}$ (as in Freudenthaler 2016; S.5.1.7).

$$\boldsymbol{I_{rot}} = \boldsymbol{R_{-45^\circ}}\boldsymbol{I} = \begin{bmatrix} I \\ U \\ -Q \\ V \end{bmatrix} \quad \textbf{Eq. 8}$$

where $\boldsymbol{R_{-45^\circ}}$ is provided in Eq. 9.

$$\boldsymbol{R_{-45^\circ}} = \begin{bmatrix} 1 & 0 & 0 & 0 \\ 0 & cos90^\circ & sin90^\circ & 0 \\ 0 & -sin90^\circ & cos90^\circ & 0 \\ 0 & 0 & 0 & 1 \end{bmatrix} = \begin{bmatrix} 1 & 0 & 0 & 0 \\ 0 & 0 & 1 & 0 \\ 0 & -1 & 0 & 0 \\ 0 & 0 & 0 & 1 \end{bmatrix} \quad \textbf{Eq. 9}$$

The light that reaches the detector is calculated as following:

$$\boldsymbol{I'_{rot,\alpha^o}} = \boldsymbol{M_{Pol.,a^\circ}}\boldsymbol{M_{PEM}}\boldsymbol{I_{rot}} = \frac{1}{2}\begin{bmatrix} I + Ucos2a - (Qcos\delta - Vsin\delta)sin2a \\ Icos2a + Ucos^2 2a - (Qcos\delta - Vsin\delta)sin2acos2a \\ Isin2a + Usin2acos2a - (Qcos\delta - Vsin\delta)sin^2 2a \\ 0 \end{bmatrix} \quad \textbf{Eq. 10}$$

Using the Bessel functions (Eq. 6), the intensity measured at the detector is provided in Eq. 11.

$$I'_{rot,\alpha^o} = \frac{1}{2}I + \left[VJ_1(A)\,sin\,\omega t - Q\left[\frac{1}{2}J_0(A) + J_2(A)\,cos\,2\omega t\right]\right]sin2a + \frac{1}{2}Ucos2a \quad \textbf{Eq. 11}$$

Measurements

Table 1 shows the measurements at the detector, as a function of a) the Stokes components, b) the linear polarizer angles and c) the rotation of the assembly.

Table 1

n	I'	Assembly without rotation	Assembly rotated at $45°$
0	DC	$\frac{1}{2}(I + Q\cos 2a + UJ_0(A)\sin 2a)$	$\frac{1}{2}(I - QJ_0(A)\sin 2a + U\cos 2a)$
1	1ωt	$VJ_1(A)\ \sin\omega t\ \sin 2a$	$VJ_1(A)\ \sin\omega t\ \sin 2a$
2	2ωt	$UJ_2(A)\cos 2\omega t\ \sin 2a$	$-QJ_2(A)\cos 2\omega t \sin 2a$

In order to have $J_0(A) = 0 \Leftrightarrow A = 2.4048 = \delta \cdot 2\pi$, thus the retardance phase shift induced by the PEM is δ = 0.382. For this value of A, $J_3(A) = 0.199$, so **there is a significant modulation at 3ωt[1], which we omit.** The intensity of the incoming sunlight, I, is calculated from the DC signal, Q is calculated (after the assembly is rotated by 45^o) from the AC signal with frequency of $2\omega t$, and U is calculated (without rotation of the assembly) from the AC signal with frequency of $2\omega t$.

$$I = I_{meas} - I_{mean,dark} \qquad \textbf{Eq. 12}$$

$I_{mean,dark}$ is the average intensity of the same-day dark measurement

The voltage output recorded at the lock-in amplifier provides Q/I, U/I as shown in the following equations:

$$v(dc) = I/2 \qquad \textbf{Eq. 13}$$

$$v(1\omega) = VJ_1(A)/\sqrt{2} \qquad \textbf{Eq. 14}$$

$$v(2\omega) = QJ_2(A)/\sqrt{2} \qquad \textbf{Eq. 15}$$

[1] Equal to $VJ_3(A)\sin(3\omega t)\sin 2a$ when the assembly is not rotated and $VJ_3(A)\sin(3\omega t)\sin 2a$ when the assembly is rotated by 45°

Multiple iris sizes test

In order to check whether there is a significant contribution to the linear polarization signal attributed to the incoming diffuse light in the instrument, we have performed a full day of tests with alternating iris sizes. The idea is that with larger iris we increase the diffused light measured by the instrument. If there is contribution of the diffused light to the measured linear polarization, then the latter should also increase with larger iris.

SolPol has a default aperture size of 5.5 mm that exactly encompasses the solar disk, provided that its tracking sequence and polar alignment are stable throughout the measurement (which we ensure before every observational sequence).

During the **25/06/2021** dust event that reached the PANGEA station, we have conducted the following test procedure (**Figure 4**):

- **alternating iris sizes** from small @**4.5 mm** to regular @**5.5 mm** to large @**7 mm** through **16'** measuring intervals so as to ensure that ambient conditions are relatively stable and that polarization does not change significantly with the instrument viewing angle.
- the **measuring sequence** is consistent with **tight** observational intervals up till the **local noon**, but then the data sequence becomes **sparse** due to failures with the assembly rotator PC communication.
- the monitored mean **AOD values** through the co-located sunphotometer do not vary significantly within the day (AOD at 440nm is approximately 0.4).
- **dark measurements** with a closed lid, closed dome and tracking mount were performed after each triplet.

The measured DOLP in Fig. 4 follows a generally decreasing trend from the morning to noon, and a generally increasing trend from noon to afternoon, due to the decreasing and increasing sun zenith angle, respectively. This is similar to the findings of (Bailey et al., 2008), with the increase of the dichroic extinction of light with increasing sun zenith angle to be an indication of possible vertical alignment of the dust particles. Figure 4 shows that this trend is disrupted when we change the size of the iris: most notably, for consecutive measurements (during morning until noon), when we decrease the iris size from 7mm to 4.5mm the DOLP increases instead of decreasing. This proves that with larger iris the DOLP is less, thus **the diffused light does not contribute to the polarization measured. This proves that the measured polarization is due to the dichroic extinction of the direct sunlight, due to the dust particle orientation.**

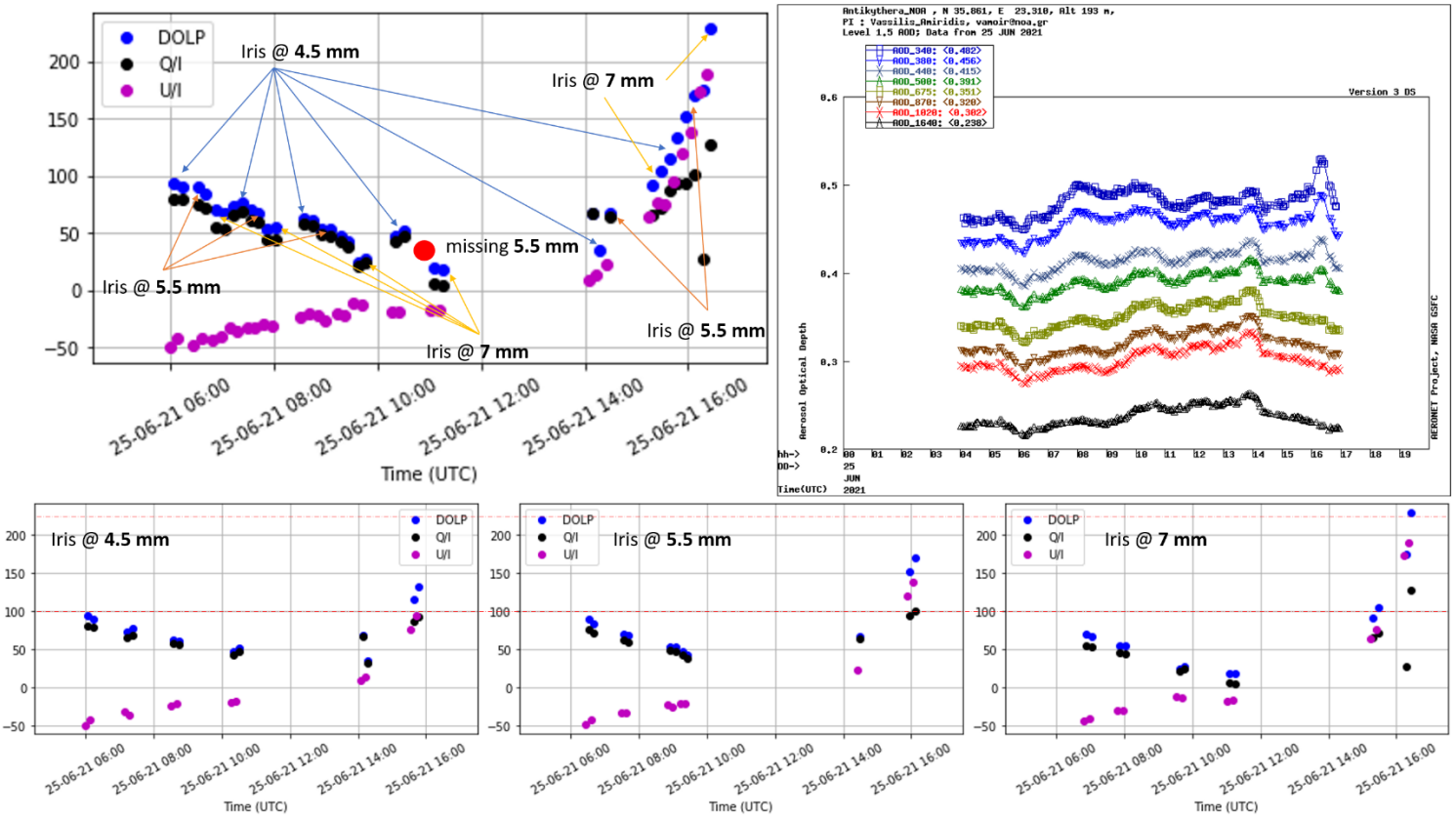

Figure 4: Measured DOLP, Q/I and U/I in ppms under consecutive iris size changes in SolPol, during the 25/06/2021 dust event. DOLP values appear to increase as the aperture closes (from 7mm to next 4.5mm) following a clearer trend in the morning as opposed to the noon measurement sequence, attributed to data sparsity.

 Instrument: *courtesy of the University of Hertfordshire*

References

Freudenthaler, V.: About the effects of polarising optics on lidar signals and the Δ90 calibration, Atmos. Meas. Tech., 9, 4181–4255, https://doi.org/10.5194/amt-9-4181-2016, 2016.

Bailey, J., Ulanowski, Z., Lucas, P. W., Hough, J. H., Hirst, E. and Tamura, M.: The effect of airborne dust on astronomical polarization measurements, Mon. Not. R. Astron. Soc., 386(2), 1016–1022, doi:10.1111/j.1365-2966.2008.13088.x, 2008.

Hough, J. H., Lucas, P. W., Bailey, J. A., Tamura, M., Hirst, E., Harrison, D. and Bartholomew-Biggs, M.: PlanetPol: A Very High Sensitivity Polarimeter, Publ. Astron. Soc. Pacific, 118(847), 1302–1318, doi:10.1086/507955, 2006.

Kemp, J. C. and Barbour, M.: A PHOTOELASTIC-MODULATOR POLARIMETER AT PINE MOUNTAIN OBSERVATORY, Publ. Astron. Soc. Pacific, 93, 521–525, 1981.

Kemp, J. C., Henson, G. D., Steiner, C. T. and Powell, E. R.: The optical polarization of the Sun measured at a sensitivity of parts in ten million, Nature, 326(6110), 270–273, doi:10.1038/326270a0, 1987.

Martin, W. E., Hesse, E., Hough, J. H., Sparks, W. B., Cockell, C. S., Ulanowski, Z., Germer, T. A. and Kaye, P. H.: Polarized optical scattering signatures from biological materials, J. Quant. Spectrosc. Radiat. Transf., 111(16), 2444–2459, doi:10.1016/j.jqsrt.2010.07.001, 2010.

Stokes, R. A., E. P. A. and S. J. B.: A New Astronomical Polarimeter, Opt. Eng., 15(1), doi:https://doi.org/10.1117/12.7971898, 1976.